Conf-760721--1

LA-UR -76-1445

TITLE: Calculations of Waves Formed from Surface Cavities

AUTHOR(S): Charles L. Mader

SUBMITTED TO: Coastal Engineering Research Council

los alamos
scientific laboratory
of the University of California
LOS ALAMOS, NEW MEXICO 87545

Form No. 836
St. No. 2629
1/75

UNITED STATES
ENERGY RESEARCH AND
DEVELOPMENT ADMINISTRATION
CONTRACT W-7405-ENG-36

CALCULATIONS OF WAVES FORMED FROM SURFACE CAVITIES

Charles L. Mader*

ABSTRACT

The wave motion resulting from cavities in the ocean surface was investigated using both the long wave, shallow water model and the incompressible Navier-Stokes equations. The fluid flow resulting from the calculated collapse of the cavities is significantly different for the two models. The experimentally observed flow resulting from explosively formed cavities is in better agreement with the flow calculated using the incompressible Navier-Stokes model. The resulting wave motions decay rapidly to deep water waves. Large cavities located under the surface of the ocean will be more likely to result in Tsunami waves than cavities on the surface. This is contrary to what has been suggested by the upper critical depth phenomenon.

I. INTRODUCTION

The prediction of water waves generated by large-yield explosions has been based on extrapolation of empirical correlations of small-yield experimental data, usually assuming the waves were shallow water waves. Because the accuracy of such predictions is questionable, the need exists for a detailed description of the mechanism by which waves are generated by explosions. In particular the "upper critical depth" phenomenon needs to be understood. The upper critical depth phenomenon is an experimentally observed wave height maximum that occurs when an explosive charge is approximately two-thirds submerged. The observed height at the upper critical depth is twice that observed for completely submerged explosive charges. If the waves formed are shallow water waves capable of forming Tsunamis, then the upper critical depth phenomenon is important to evaluating the probability of a Tsunami event from other than tectonic events.

Theoretical evaluation of the early interaction of the detonation products of an explosive charge with the water and air interfaces and the resulting wave profile near the detonation has been performed by Mader[1] using the multicomponent reactive compressible hydrodynamic code 2DE.[2] The pressure and velocity contours for the early interaction of the explosive with the water and air are shown in Fig. 1. The initial formation of the lip or splash wave on the water cavity is also numerically described and it has been suggested that the concentration of momentum near the water surface in the splash wave is a contributing

*Theoretical Division, Los Alamos Scientific Laboratory, University of California, Los Alamos, New Mexico 87545

factor in the upper critical depth phenomenon, resulting in a bubble cavity radius about the same as if the explosive bubble was completely confined by water. The high velocity present in the splash wave is a result of the initial water shock being quickly rarefied and permitting a second shock to be delivered from the explosive products. Subsequent shocks and rarefactions occur while the detonation products have high pressure. Each reverberation increases the particle velocity of the splash wave by an increment that decreases as the pressure of the driving detonation products decreases. The particle velocity of the remainder of the water cannot be increased by reverberations during the early high pressure motion because a free interface is not present. The consequence of this complicated interaction is that the maximum bubble radius achieved by a partially submerged explosive charge is slightly larger than one would expect to observe if the explosive sphere and its bubble was confined by water at one bar.

The bubble is observed to increase to a maximum radius of about 0.5 meter in 0.2 second and then take about 0.3 second to collapse as described in Refs. 1 and 3 for a 1.27-cm radius 9404 explosive sphere initiated at the center and immersed to a depth of 1.59 cm.

In this paper we shall describe an investigation of the flow after the cavity reaches its maximum dimensions. We assume that the flow is essentially incompressible at the times of interest and that the surrounding fluid is approximately at rest at maximum bubble radius.

The waves observed by Craig[3] from the collapse of the bubble resulted in a train of waves moving at about 1.25 meters/second with a one-meter wavelength. Mass markers located one meter below the water surface and markers located half a meter below the surface and one meter from the explosive did not show any appreciable movement compared with those located nearer the surface or explosive charge. This result suggests that the fluid flow will not be well described by the usual shallow water-long wave model.

We have calculated the fluid dynamics of a cavity initially 0.5 meter in radius with and without a lip, using a shallow water long wave model and a model based upon the incompressible Navier-Stokes equations.

II. SHALLOW WATER, LONG WAVE MODEL

The long wave theory applies when the depth relative to the wavelength is small, and when the vertical component of the motion does not influence the pressure distribution, which is assumed to be hydrostatic. It is appropriate for Tsunami wave formation, propagation and early shoaling behavior as described in Ref. 4. The SWAN code described in Ref. 4 was modified to solve the long wave equations using an improved numerical difference technique.

The long wave equations solved by the SWAN code are:

$$\frac{\partial U}{\partial t} + U\frac{\partial U}{\partial X} + V\frac{\partial U}{\partial Y} + g\frac{\partial H}{\partial X} = FV + F^{(x)} - g\frac{U(U^2 + V^2)^{1/2}}{C^2(D + H)}$$

$$\frac{\partial V}{\partial t} + U\frac{\partial V}{\partial X} + V\frac{\partial V}{\partial Y} + g\frac{\partial H}{\partial Y} = FU + F^{(y)} - g\frac{U(U^2 + V^2)^{1/2}}{C^2(D + H)}$$

$$\frac{\partial H}{\partial t} + \frac{\partial(D + H - R)U}{\partial X} + \frac{\partial(D + H - R)V}{\partial Y} - \frac{\partial R}{\partial t} = 0$$

where U = velocity in X direction (i index)
V = velocity in Y direction (j index)
g = gravitational acceleration
t = time (n index)
H = wave height above mean water level
R = bottom motion
F = Coriolis force parameter
C = coefficient of DeChezy for bottom stress
$F^{(x)}$, $F^{(y)}$ = forcing functions of wind stress and barometric pressure in X and Y direction
D = depth .

To obtain stable numerical solutions, the finite difference equations must not have negative diffusion. The following difference equations are stable but require that the time step be kept near the maximum or the numerical results will become smeared. C. W. Hirt[5] suggested this approach when the difference equations described in Ref. 4 were found to be unstable in certain directions of the flow.

The wave height H and depth D are taken as cell centered and the velocities are centered at cell boundaries. The difference equations at each time step are in order:

$$H^{n+1}_{i,j} = H^n_{i,j} - \Delta t\left[\frac{U^n_{i+1,j}}{\Delta x}(TD1) - \frac{U^n_{i,j}}{\Delta x}(TD2) + \frac{V^n_{i,j+1}}{\Delta y}(TV1) - \frac{V^n_{i,j}}{\Delta y}(TV2)\right]$$

$$+ R^{n+1}_{i,j} - R^n_{i,j}$$

$$TD1 = D_{i+1,j} + H^n_{i+1,j} - R^n_{i+1,j} \quad (U_{i+1,j} < 0)$$

$$TD2 = D_{i,j} + H^n_{i,j} - R^n_{i,j} \quad (U_{i,j} < 0)$$

$$TV1 = D_{i,j+1} + H^n_{i,j+1} - R^n_{i,j+1} \quad (V_{i,j+1} < 0)$$

$$TV2 = D_{i,j} + H^n_{i,j} - R^n_{i,j} \quad (V_{i,j} < 0)$$

$$TD1 = D_{i,j} + H^n_{i,j} - R^n_{i,j} \quad (U_{i+1,j} > 0)$$

$$TD2 = D_{i-1,j} + H^n_{i-1} - R^n_{i-1,j} \quad (U_{i,j} > 0)$$

$$TV1 = D_{i,j} + H^n_{i,j} - R^n_{i,j} \quad (V_{i,j+1} > 0)$$

$$TV2 = D_{i,j-1} + H^n_{i,j-1} - R^n_{i,j-1} \quad (V_{i,j} > 0)$$

$$U^{n+1}_{i,j} = U^n_{i,j} - \Delta t \left[\frac{U_{i,j}}{\Delta x} (TU1) + \frac{TV}{\Delta Y} (TU2) \right] - g \frac{\Delta t}{\Delta x} [THU]$$

$$+ \Delta t \left\{ -FV^n_{i,j} - F^{(x)}_{i,j} + S^B_{i,j} \right\}$$

$$TV = 0.25 \, (V_{i,j} + V_{i,j+1} + V_{i-1,j+1} + V_{i-1,j})$$

$$TU1 = U_{i+1,j} - U_{i,j} \quad (U_{i,j} < 0)$$

$$TU2 = U_{i,j+1} - U_{i,j} \quad (TV < 0)$$

$$TU1 = U_{i,j} - U_{i-1,j} \quad (U_{i,j} > 0)$$

$$TU2 = U_{i,j} - U_{i,j-1} \quad (TV > 0)$$

$$THU = H_{i,j} - H_{i-1,j}$$

$$V^{n+1}_{i,j} = V^{n}_{i,j} - \Delta t\left[\frac{TU}{\Delta X}(TV1) + \frac{V_{i,j}}{\Delta Y}(TV2)\right] - g\,\frac{\Delta t}{\Delta Y}[THV]$$

$$+ \Delta t\left\{FU^{n}_{i,j} - F^{(y)}_{i,j} + S^{B}_{i,j}\right\}$$

$$TU = 0.25\,(U_{i,j} + U_{i+1,j} + U_{i,j-1} + U_{i+1,j-1})$$

$$TV1 = V_{i+1,j} - V_{i,j}\ (TU < 0)$$

$$TV2 = V_{i,j+1} - V_{i,j}\ (V_{i,j} < 0)$$

$$TV1 = V_{i,j} - V_{i-1,j}\ (TU > 0)$$

$$TV2 = V_{i,j} - V_{i,j-1}\ (V_{i,j} > 0)$$

$$THV = H_{i,j} - H_{i,j-1}$$

and

$$S^{B}_{i,j} = gU^{n}_{i,j}\left(\overline{U^{n}_{i,j}}^{2} + \overline{V^{n}_{i,j}}^{2}\right)^{1/2} \Big/ C^{2}\left(D_{i,j} + H^{n}_{i,j}\right) \quad .$$

The calculations were performed with 69 cells in the X direction and 130 cells in the Y direction. The cells were .06 meters square and the time step was 0.001 seconds. The gravity constant was -9.8 m sec^{-2}. Although the problem described in this report was symmetrical and required only one direction, the calculations described were performed with the two dimensional SHAL code.

The computed wave profiles using the shallow water equations in the SHAL code for the collapse of a 0.5-meter radius hole are shown in Fig. 2 and for the collapse of a 0.5-meter radius hole with a 0.25-meter high and 0.50-meter wide triangular lip (which approximates the experimentally observed bubble profile) are shown in Figs. 2 and 4. Figure 4 also shows the velocity in the Y direction. The initial water depth was three meters.

III. INCOMPRESSIBLE NAVIER-STOKES MODEL

The Marker and Cell (MAC) method of Harlow and Welch[6] is a numerical technique for calculation of viscous, incompressible flow with a free surface.

The method uses a finite-difference technique for solving the time-dependent Navier-Stokes equations.

These equations for two-dimensional flows are

$$\frac{\partial U}{\partial X} + \frac{\partial V}{\partial Y} = 0 \quad ,$$

$$\frac{\partial U}{\partial t} + \frac{\partial U^2}{\partial X} + \frac{\partial UV}{\partial Y} = - \frac{\partial \phi}{\partial X} + g_X + \nu \left(\frac{\partial^2 U}{\partial X^2} + \frac{\partial^2 U}{\partial Y^2} \right) \quad ,$$

$$\frac{\partial V}{\partial t} + \frac{\partial UV}{\partial X} + \frac{\partial V^2}{\partial Y} = - \frac{\partial \phi}{\partial Y} + g_Y + \nu \left(\frac{\partial^2 V}{\partial X^2} + \frac{\partial^2 V}{\partial Y^2} \right) \quad ,$$

where ϕ is the ratio of pressure to constant density, g_X and g_Y are the X and Y components of body acceleration, and ν is the kinematic viscosity coefficient. The MAC method is based on an Eulerian network of rectangular cells, with velocities centered at cell boundaries and the pressure cell-centered. Just as the differential equations of motion are statements of the conservation of mass and momentum, the MAC finite-difference equations express these conservation principles for each cell, or combination of cells, in the computing mesh.

After the introduction of MAC, much attention was given to devising more accurate treatments of the free surface boundary conditions. Chan and Street[7] developed a technique for more accurate delineation of the free surface. This permitted the free surface pressure to be specified at the surface itself, rather than at the center of the surface cell. Nichols and Hirt[8] modified the Chan and Street procedure, devising a technique for defining the fluid surface by a set of surface marker particles that move with local fluid velocity. These particles allow surface-cell pressures in MAC to be accurately specified by means of linear interpolation or extrapolation between the known values of pressure in the nearest full cell and the desired fluid surface.

A Simplified MAC (SMAC) has been described by Harlow and Amsden.[9] The SMAC technique has been modified to include the Nichols and Hirt free surface treatment. The computing program used for the calculations is called ZUNI and is described by Amsden.[10] The calculations were performed with 100 cells in the X direction and 60 cells in the Y direction. The cells were 0.05 meters square and the time step increment was 0.0003 seconds. The convergence criterion is the maximum permitted change in pressure from hydrostatic pressure in any cell between iteration steps divided by the sum of the changes at two iteration steps and was 0.01. Three or more surface particles were used in each cell. The gravity constant was -9.8 m sec^{-2}. The viscosity coefficient was 0.01 gm sec^{-1} m^{-1}. Preliminary calculations showed that the results were independent of whether the water depth was 3.0 or 1.5 meters; therefore in the calculations presented in this paper the cavity was in

water initially 1.5 meters deep. The wave amplitude at late times and the details of the bubble collapse after first collapse and jetting were sensitive to the amount of viscosity used in the calculation so the value chosen was the smallest that would also permit numerically stable results. The computed wave profiles using the ZUNI code to solve the incompressible Navier-Stokes equations for the collapse of a 0.5-meter radius hole with a 0.25-meter high and 0.5-meter wide triangular lip are shown in Fig. 5.

IV. COMPARISONS

The experimental and calculated wave parameters are summarized in Table I. The experimental wave parameters are given for the first three waves after four meters of travel from the center of the explosive charge. The calculated wave parameters for the Airy wave were calculated using the WAVE code* for a depth of three meters and using the experimentally observed wave height and wave length. Since the group velocity is almost exactly half the wave velocity, the Airy wave is a deep water wave. The deep water Airy wave is a good approximation to the experimentally observed wave.

The collapse of the cavity is quite different between the SHAN and ZUNI calculation as shown in Figs. 3 and 5. The shallow water cavity calculation collapses from the side in less than 0.1 second while the Navier-Stokes cavity calculation collapses from the bottom in about 0.5 seconds. The experimentally observed bubble collapses approximately symmetrically from the bottom in about 0.3 seconds, so the Navier-Stokes calculation is a more realistic description of the observed flow.

As shown in Table I the Navier-Stokes calculation results in wave parameters more closely approximating those observed experimentally than those calculated using the shallow water theory. The waves calculated using the incompressible Navier-Stokes equations have complicated wave patterns and the waves quickly decay into deep water waves with the particle motion rapidly decreasing with increasing depth below the water surface. This is also in agreement with the experimental observations of mass markers described in the introduction.

TABLE I

CALCULATED AND EXPERIMENTAL WAVE PARAMETERS

	Experimental*	Airy Wave	Shallow Water	Navier-Stokes
Wave Velocity (m/s)	1.25 ± 0.1	1.2489	5.42	1.50 ± 0.50
Amplitude (cm)	1, 1.8, 2.5	2.5 (input)	10.1	< 4.0
Wave Length (m)	1.5, 1.0, 1.0	1.0 (input)	1.0	1.0
Period (s)	1.2, 0.8, 0.8	0.8007	0.18	$0.66^{+0.3}_{-0.2}$
Group Velocity (m/s)		0.6244		

*First three waves observed.

V. CONCLUSIONS

The experimentally observed waves from the cavities formed by explosions near the water surface are better reproduced by models solving the incompressible Navier-Stokes equations than by models solving the shallow water, long wave equations. The experimentally observed waves are deep water waves and the observed upper critical depth phenomenon is apparently a result of a partition of energy near the water surface which results in high amplitude deep water waves (of high potential and low kinetic energy) and not the shallow water waves required for Tsunamis. As the explosive is detonated under the water surface, more of the energy is imparted to the water resulting in waves that have smaller amplitude but more of the energy is present in the water as kinetic energy rather than potential energy. The waves formed will more closely resemble shallow water waves and will not disperse as rapidly as waves formed from surface detonation.

The upper critical depth phenomenon is apparently not important to the formation of Tsunami waves. Large cavities located under the surface of the ocean will be more likely to result in shallow water Tsunami waves than cavities on the surface. A cavity would have to be quite large and reach very deep into the ocean before it could be an effective agent for forming significant Tsunami waves.

To obtain a more realistic solution to the problem of wave formation from explosions one would need to follow the hydrodynamics from the early compressible to late incompressible stages with one of the implicit continuous fluid methods currently under development. Of particular interest would be to determine the source and significance for wave formation of the water jet and root experimentally[3] observed before the explosive bubble reaches maximum radius at depths similar to the upper critical depth.

ACKNOWLEDGMENTS

The author gratefully acknowledges the contributions of A. A. Amsden, F. H. Harlow, B. D. Nichols, T. D. Butler, C. W. Hirt, and K. H. Olsen of the Los Alamos Scientific Laboratory, of G. R. Miller, H. G. Loomis, and E. N. Bernard of the Joint Tsunami Research Effort, National Oceanic and Atmospheric Administration, Hawaii Institute of Geophysics, and of George Carrier of Harvard University.

This study was performed for the Energy Research and Development Administration Tamarin Committee.

LITERATURE CITED

1. Charles L. Mader, "Detonations Near the Water Surface," Los Alamos Scientific Laboratory report LA-4958 (1972).

2. James D. Kershner and Charles L. Mader, "2DE: A Two Dimensional Continuous Eulerian Hydrodynamic Code for Computing Multicomponent Reactive Hydrodynamic Problems," Los Alamos Scientific Laboratory report LA-4932 (1972).

3. Bobby G. Craig, "Experimental Observations of Underwater Detonations Near the Water Surface," Los Alamos Scientific Laboratory report LA-5548-MS (1974).

4. Charles L. Mader, "Numerical Simulation of Tsunamis," Hawaii Institute of Geophysics report HIG-73-3 and Joint Tsunami Research Effort report NOAA-JTRE-85 (1973), also J. Physical Oceanography 4, 74-82 (1974).

5. C. W. Hirt, private communication.

6. J. E. Welch, F. H. Harlow, J. P. Shannon and B. J. Daly, "The MAC Method," Los Alamos Scientific Laboratory report LA-3425 (1965).

7. R. K. C. Chan and R. L. Street, J. Comput. Phys. 6, 68-94 (1970).

8. B. D. Nichols and C. W. Hirt, J. Comput. Phys. 8 434-448 (1971).

9. Anthony A. Amsden and Francis H. Harlow, "The SMAC Method: A Numerical Technique for Calculating Incompressible Fluid Flows," Los Alamos Scientific Laboratory report LA-4370 (1970), also J. Comput. Phys. 6 322-325 (1970).

10. Anthony A. Amsden, "Numerical Calculation of Surface Waves: A Modified ZUNI Code with Surface Particles and Partial Cells," Los Alamos Scientific Laboratory report LA-5146 (1973).

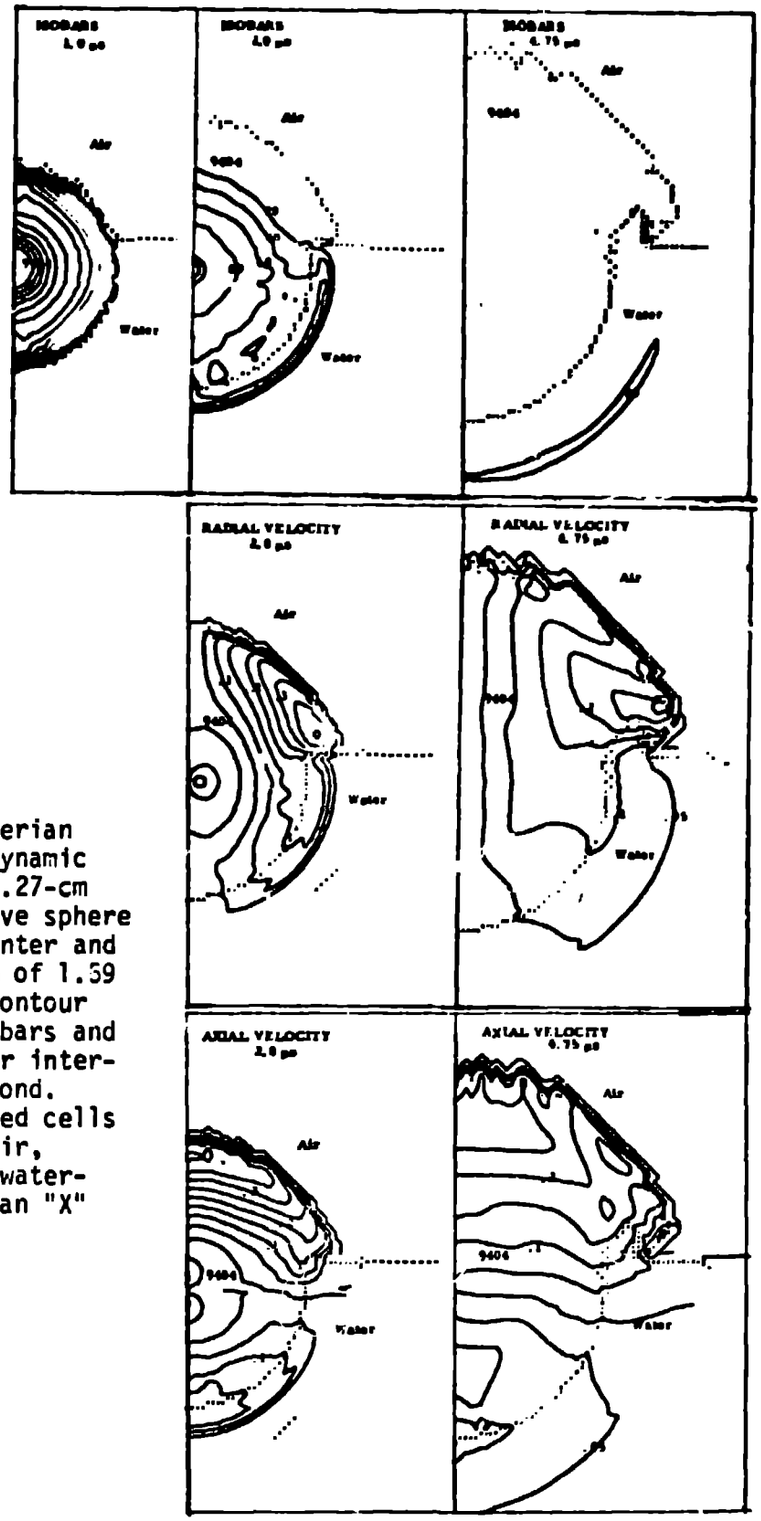

Fig. 1. Two-dimensional Eulerian compressible hydrodynamic calculations of a 1.27-cm radius 9404 explosive sphere initiated at its center and immersed to a depth of 1.59 cm. The pressure contour interval is 20 kilobars and the velocity contour interval is 0.05 cm/μsecond. The position of mixed cells (9404-water, 9404-air, water-air, or 9404-water-air) is shown with an "X" plotting symbol.

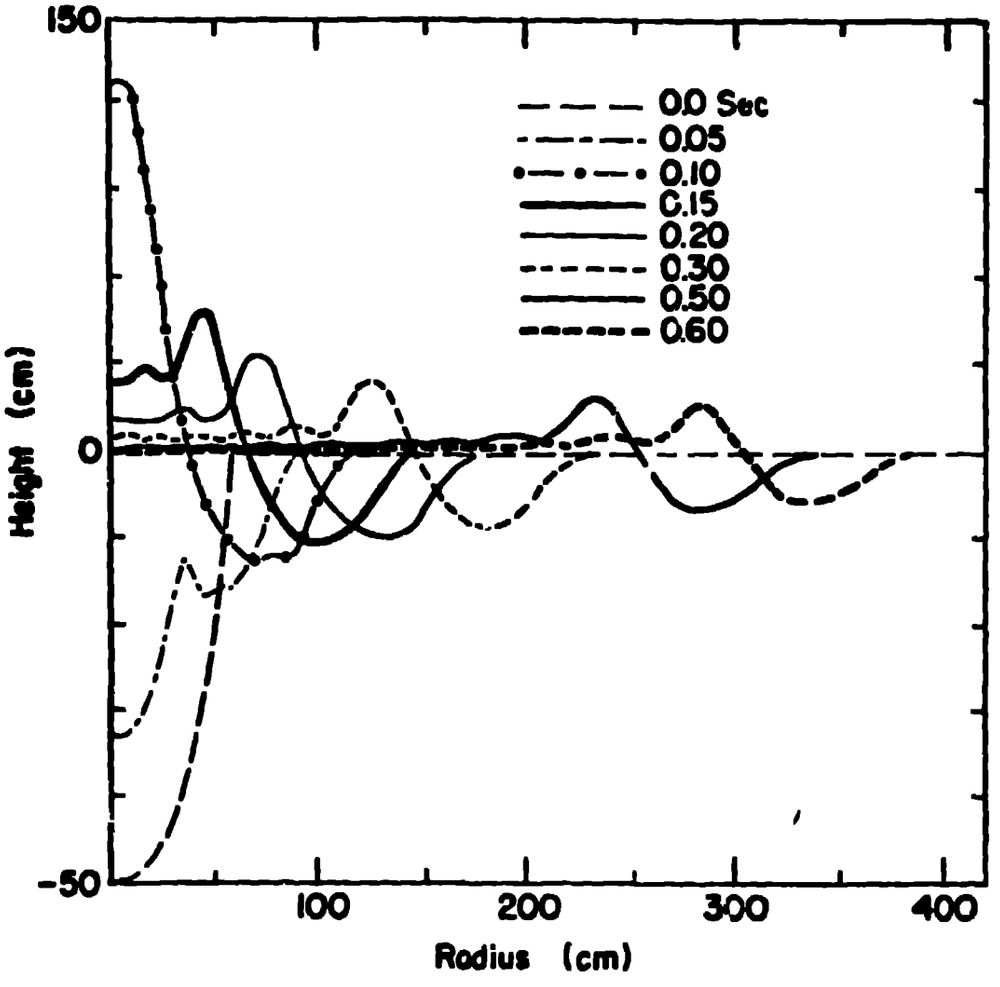

Fig. 2. The computed surface height vs radius at various times of the collapse of a 50-cm radius hole in three meters of water using the shallow water-long wave model and the SWAN code.

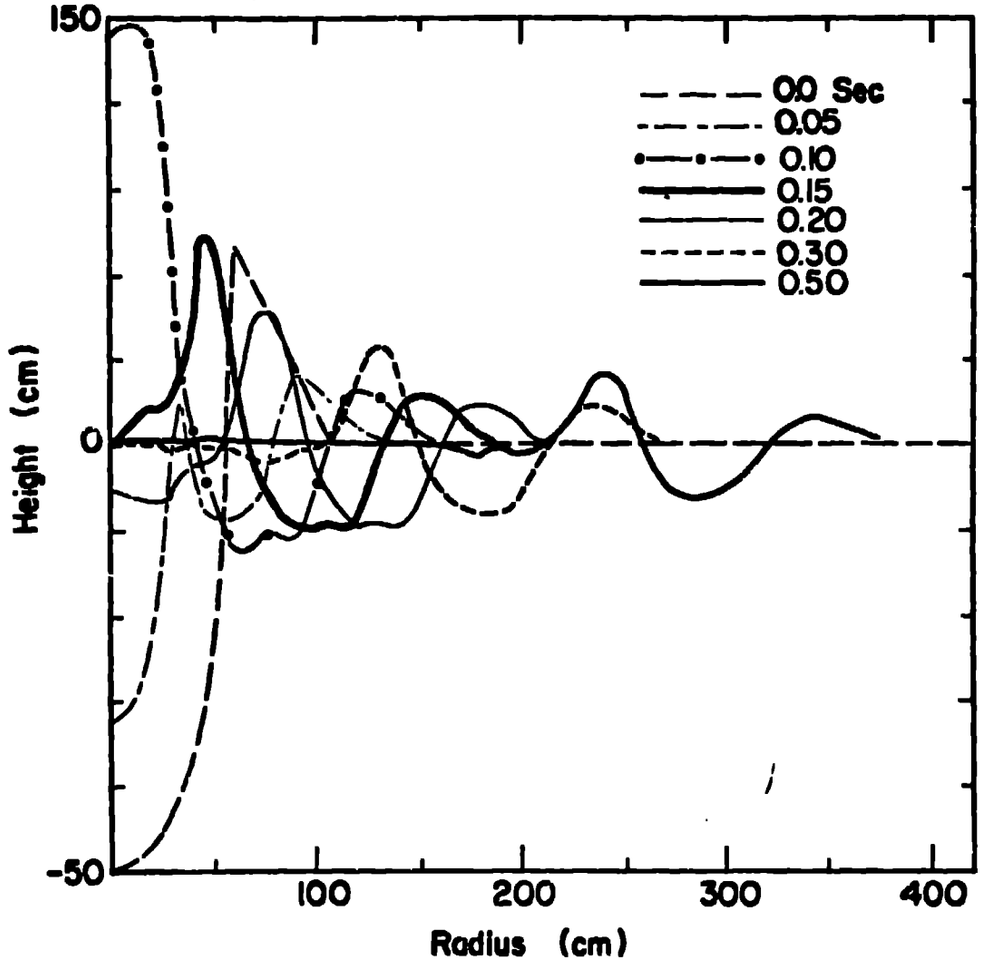

Fig. 3. The calculated surface height vs radius at various times of the collapse of a 50-cm radius hole with a triangular lip using the shallow water-long wave model and the SWAN code.

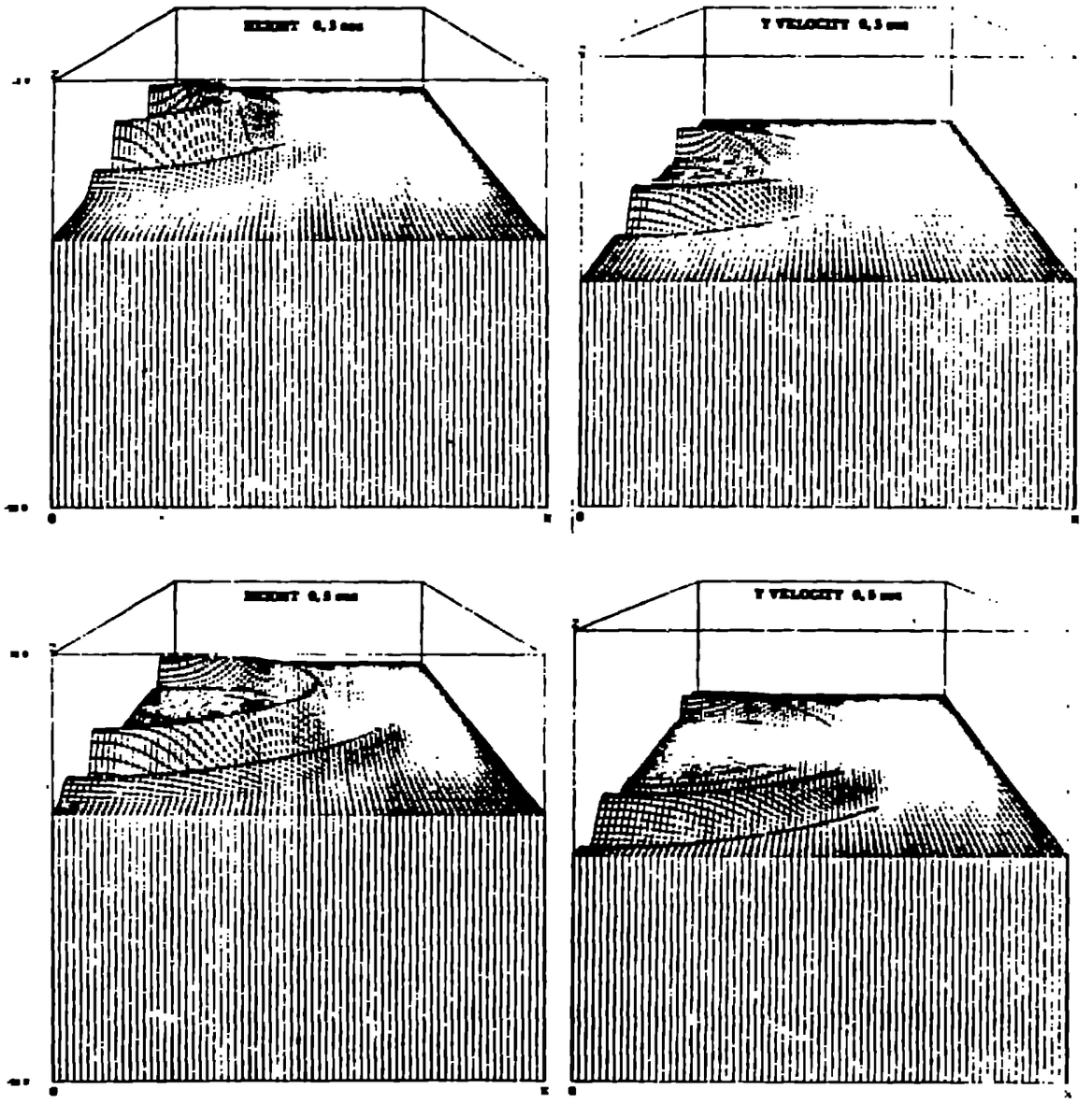

Fig. 4. Picture plots in three dimensions of the surface profiles and the velocity in the Y direction profiles at 0.3 and 0.5 seconds for the calculation described in Fig. 3.

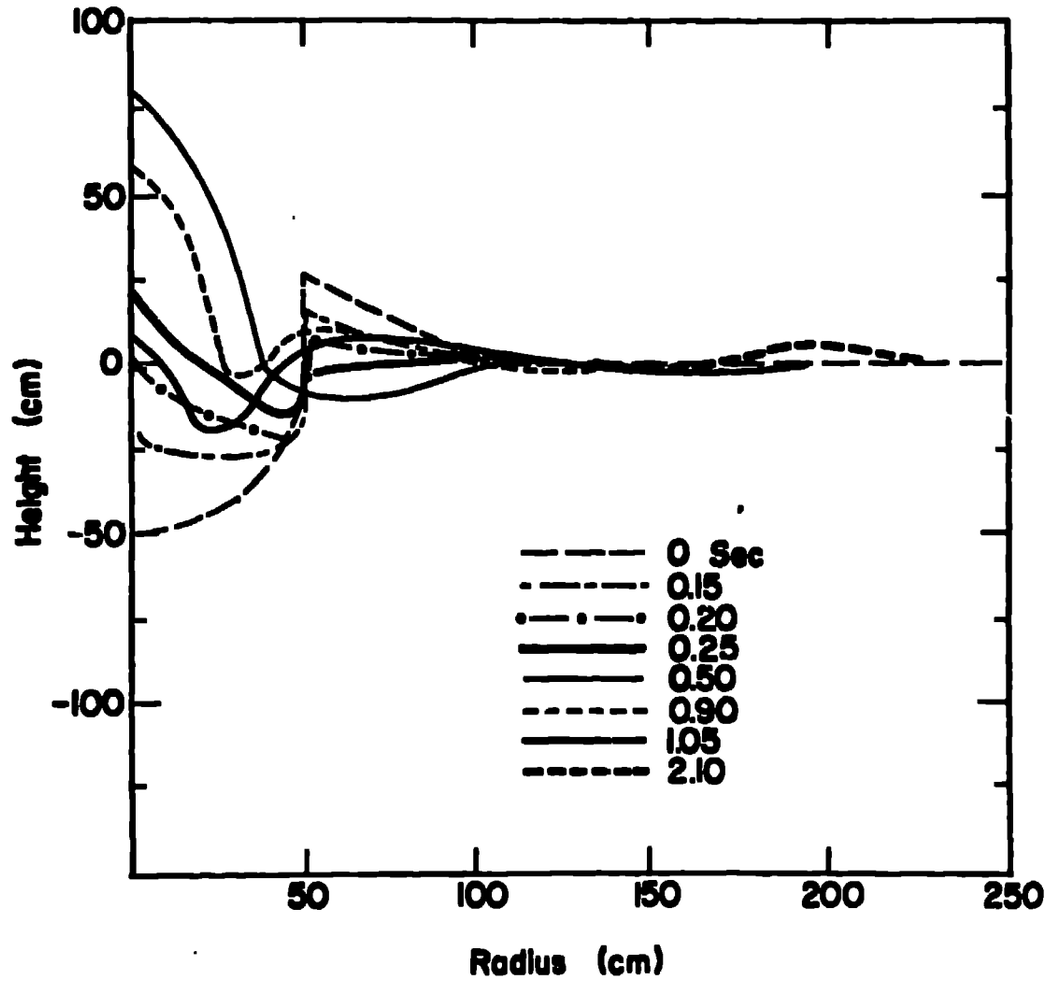

Fig. 5. The calculated surface height vs radius at various times of the collapse of a 50-cm radius hole with a triangular lip using the incompressible Navier-Stokes model and the ZUNI code.